THE ASTROPHYSICAL JOURNAL, 460:L99–L102, 1996 April 1

DETERMINING THE GAMMA-RAY BURST DISTANCE SCALE: OBSERVATIONAL PROSPECTS

FIONA A. HARRISON[1]
Space Radiation Laboratory, California Institute of Technology, Pasadena, CA 91125

AND

S. E. THORSETT[2]
Joseph Henry Laboratories and Department of Physics, Princeton University, Princeton, NJ 08544

Received 1995 July 21; accepted 1996 January 19

ABSTRACT

The BATSE instrument on the *Compton Gamma-Ray Observatory* has demonstrated that we live near the center of an isotropic but bounded distribution of gamma-ray burst sources but has left unsettled whether the bursts occur in our own Galaxy or at cosmological distances. Because a distance and energy scale is crucial to constraining burst models, this distance ambiguity must be resolved. The key experiment that would distinguish the possibilities is a search for bursts from the halo of M31 or other nearby galaxies. We discuss the observational prospects for this test, showing that no telescope now in orbit or scheduled for launch can settle the debate, but that an experiment could be done with a low-cost, dedicated instrument.

Subject headings: Galaxy: halo — gamma rays: bursts — stars: neutron

1. INTRODUCTION

Gamma-ray bursts (GRBs) were discovered by the first small gamma-ray satellites placed in orbit, nearly 30 years ago. Despite enormous advances in observational sophistication since then, the origin of these mysterious high-energy events remains unknown. The Burst and Transient Source Experiment (BATSE) on the *Compton Gamma-Ray Observatory* has made significant progress by a strategy of high-sensitivity burst observations with nearly uniform sky coverage. The isotropy of its large sample of GRBs, together with its confirmation that there are fewer faint bursts than expected for an isotropic distribution, rule out the hypothesis that bursts arise on the surfaces of nearby (disk population) neutron stars. Instead, the observations are consistent with either an extended Galactic halo (often referred to as a corona to distinguish it from the classical Galactic halo) (Lamb 1995) or a cosmological (Paczyński 1995) origin.

The simplest way to distinguish galactic and extragalactic burst distributions is to search for similar halos around other galaxies. The fact that BATSE does not observe an excess of bright bursts in the direction of M31 already gives an outer limit to the BATSE sampling distance and an upper limit to burst fluxes in a galactic model (Hakkila et al. 1994). Because a lower limit on the characteristic distance to BATSE's weakest bursts comes from the apparent isotropy of the bursts despite the solar system's offset from the Galactic center, one can estimate for any galactic model how much more sensitive than BATSE an instrument must be before M31 will be detectable.

In this Letter, we first review the current distance limits on GRBs (§ 2). In § 3 we discuss the technical aspects of detecting bursts fainter than the BATSE threshold. In § 4, we show the limits of existing satellites and describe how a simple, dedicated instrument could settle the GRB distance scale question.

[1] E-mail: fiona@srl.caltech.edu.
[2] E-mail: steve@pulsar.princeton.edu.

2. CURRENT LIMITS ON THE DISTANCE SCALE

The BATSE observations (Fishman et al. 1994) force two important constraints on the GRB source distribution: the burst sources must be nearly isotropically distributed, and the number of bursts N brighter than a flux S must increase as $N \propto S^{-0.8}$ for faint bursts, significantly flatter than the $N \propto S^{-1.5}$ expected for a homogeneous distribution and observed for the brighter sample of bursts detected by the *Pioneer Venus Orbiter* (Chuang et al. 1992). The simplest conclusion is that we observe GRBs from near the center of a spherically symmetric but bounded distribution. This is naturally understood if the bursts are at cosmological distances, with the rolloff due to evolution or the cosmological curvature of space. Models that place bursts in an extended halo around the Galaxy naturally account for the boundedness of the distribution but would predict a measurable dipole moment toward the Galactic center unless the bursts are in an unusual distribution, with typical bursts seen by BATSE at galactocentric radii $d \gtrsim 100$ kpc.

A Galactic GRB distribution is often parameterized with a form appropriate for the dark matter halo:

$$\rho(r) \propto \frac{1}{1 + (r/r_c)^{\alpha}}, \qquad (1)$$

where r_c is the core radius and $\alpha = 2$ for an asymptotically flat rotation curve. Assuming this distribution and that all bursts have the same peak flux (the "standard candle" assumption), the BATSE angular moment and luminosity constraints imply that BATSE is observing bursts to a distance between 150 and 400 kpc, depending on r_c and α (Hakkila et al. 1994). It is possible that the distribution deviates significantly from equation (1). It is relatively easy to construct models consistent with isotropy if the outer halo is not spherically symmetric (Podsiadlowski, Rees, & Ruderman 1995). Although the luminosity constraints have not yet been considered for these models, the general result that the characteristic distance to BATSE's weakest bursts is $\gtrsim$150 kpc still applies.

The upper limit on the distance of the BATSE bursts in Galactic halo models comes from BATSE's nonobservance of

an excess of bursts toward our nearest neighbor spiral galaxy, M31, at a distance $D_{M31} \sim 700$ kpc (Cohen 1985). If R_{samp} is BATSE's sampling distance ($\gtrsim$150 kpc), achieving a high burst detection rate for bursts from M31 requires an instrument $(D_{M31}/R_{samp})^2 \sim 20$ times more sensitive than BATSE. Of course, some bursts will be detected first from the near side of M31's halo, but the number depends on extrapolation of the halo distribution beyond R_{samp}, and at threshold M31 will appear as a very low surface brightness enhancement over a very large angular diameter.

3. OBSERVING BURSTS BEYOND THE BATSE LIMIT

As deeper observations are made, coronal models predict that enhancements due to other galaxies in the burst angular density will become apparent. M31 will appear first, as an enhancement subtending 20°–60° on the sky. At fainter flux levels additional, more concentrated excesses due to galaxies at larger distances will become visible. The detectability of these density fluctuations depends on the depth of the exposure and the fraction of sky observed.

The statistical detection significance for burst detection (the ratio of signal counts to expected fluctuations in the background counts) for an X-ray or gamma-ray telescope is given by

$$K = \frac{FA_{coll}}{\sqrt{BA_{cell}}}, \quad (2)$$

where the detected source and background counts per unit area are given by

$$F = \int_0^{t_0} \int_{E_1}^{E_2} f(E, t)\epsilon(E)\, dE\, dt, \quad B = \int_{E_1}^{E_2} t_0 b(E)\, dE, \quad (3)$$

$f(E, t)$ and $b(E)$ are the incident burst flux and background in photons cm^{-2} s^{-1} keV^{-1}, $\epsilon(E)$ is the instrument detection efficiency, A_{coll} is the instrument geometric collecting area, A_{cell} is the area of the detector cell over which the source flux gets concentrated, t_0 is the timescale over which the burst flux is integrated, and the detector operates over the energy band $E_1 < E < E_2$. Where BA_{cell} is small (as for focusing instruments), a constant search threshold based on systematics rather than background fluctuations replaces BA_{cell}. For a BATSE large area detector (LAD), $A_{coll} = A_{cell} = 2000$ cm^2, $E_1 = 50$ keV, $E_2 = 300$ keV, and $t_0 = 0\overset{s}{.}064$, $0\overset{s}{.}256$, or $1\overset{s}{.}024$. To detect bursts fainter than BATSE, there are several possible approaches.

The first is to increase A_{coll}. For a typical, nonfocusing, hard X-ray/gamma-ray instrument in Earth orbit, A_{coll} is approximately equivalent to the detector area, and burst detection at the flux threshold is background limited. In this limit, $A_{cell}/A_{coll} \approx 1 \gg F/B$, so $K \propto A_{coll}^{1/2}$. Hence a factor of 10 increase in area yields only a factor ~3 sensitivity improvement.

In the background-limited regime, $K \propto B^{-1/2} \propto b^{-1/2}$, so a second option is to reduce b, by collimation or shielding. Collimation reduces background at energies where the diffuse cosmic contribution dominates, while shielding improves detection significance at higher energies where internal background dominates. BATSE was designed for all-sky coverage, but searching for burst coronae from other galaxies can be done over more limited fields of view (FOVs), making fainter flux levels more easily obtainable.

BATSE triggers on burst flux in the energy range 50–300 keV. Improved sensitivity to bursts can also be achieved by extending spectral coverage with high detection efficiency to energies less than 50 keV. The BATSE detection efficiency peaks at 100 keV, decreasing below this energy. Both burst spectra and the diffuse flux change spectral shape in the 10–100 keV band, and the sensitivity advantage depends on the burst spectrum. By folding a sample of burst spectra characterized by Band et al. (1993) through various instrument responses, we found that extending detection efficiency to less than 50 keV decreases the detection threshold for an instrument with a background dominated by cosmic diffuse flux.

Focusing X-ray telescopes have been proposed as a means of detecting distant bursts (Liang 1991). Focusing instruments gain sensitivity by concentrating the source flux on a small region of the detector, greatly reducing the background. The ratio A_{cell}/A_{coll} in equation (2) can be as small as 10^{-3}, so that observations can be signal-limited down to much lower fluxes.

Many bursts observed by BATSE have durations in excess of 10 s, much longer than the longest BATSE trigger timescale ($1\overset{s}{.}024$). By including timescales up to 50 s in the trigger, long-duration bursts can be detected at fainter flux levels. Temporal variation in background rates over these timescales must, however, be minimal. In general, this requires additional background rejection and collimation over what BATSE achieves.

It is important to note that the diversity of GRB spectra and timescales preclude a unique measure of the relative instrumental sensitivity for experiments with different spectral and temporal response. Bursts which appear to be standard candles using one instrumentally defined flux measure will not appear so to an experiment with different spectral or temporal response. It is therefore necessary to define relative sensitivity for a statistical sample of bursts (see § 4).

4. EXPERIMENTAL APPROACHES TO DEEP BURST SEARCHES

The expected number of excess bursts in the direction of a particular galaxy, expressed in terms of the relevant observational parameters, is given by

$$N = MN_G T\epsilon_{obs} F_D, \quad (4)$$

where N_G is the number of bursts per year in the Milky Way, T is the observation time, ϵ_{obs} is the observational duty cycle, M is the ratio of the mass of the galaxy to the mass of the Milky Way, and F_D is the fraction of the burst halo that is detectable by the given instrument. Expressed as an integral along the line of sight, z,

$$F_D = \int_{FOV} d\Omega \int_{z_{min}}^{z_{max}} f_d(z) n(z, \rho) z^2\, dz. \quad (5)$$

In this expression, f_d is the fraction of bursts above the instrument detection threshold, $n(z, \rho)$ is the burst number density per unit volume normalized to unity over the entire halo, and ρ is the angular distance from the center of the galaxy, which is assumed to be small enough that spherical projection effects can be ignored.

The total number of bursts in the galaxy, the burst radial density distribution, and the luminosity function are unknown but are constrained by the observed angular isotropy and lnN-lnS distributions. Under the assumption that the BATSE sample of bursts is representative of the entire burst population, the number of bursts detectable by a given instrument for a particular model halo surrounding M31 can be determined by folding a sample of BATSE burst spectra and time profiles through the instrument response, with the flux normalizations determined by the model radial distribution and luminosity

function. Of course, the BATSE bursts may not be representative of the total burst population, and instruments with different response may be sensitive to bursts with distributions different from those measured by BATSE. Burst rates based on the BATSE measurements are not exact and must be considered representative of the expected rates. We emphasize that a control observation must be performed to determine the burst rate away from M31 for any instrument with spectral or temporal response different from BATSE.

Discussion of the detection rates from all halo radial distributions and burst luminosity functions consistent with the BATSE data is beyond the scope of this Letter. Rather, in order to illustrate the observational considerations, we adopt the common assumptions of standard candle burst luminosities and halo radial distributions given by equation (1). Given this simplification and the uncertainties introduced by the instrumental selection effects, we emphasize that the resulting burst rates are representative and, for example, may be underestimated for instruments with better low-energy response than BATSE and for models with a distribution of intrinsic luminosities. For halo distributions consistent with equation (1), introducing an intrinsic luminosity function tends to decrease the range of allowed $R_{\rm samp}$, at the same time increasing the number of intrinsically brighter bursts (Hakkila et al. 1994). The overall result is to make a larger fraction of bursts from M31 detectable.

4.1. *Experiment Sensitivities*

Using the assumptions of standard candle burst luminosities (specifically that all bursts emit the same photon flux in the 50–300 keV BATSE trigger band) and that the total burst population is represented by the BATSE sample, we have calculated f_d for a variety of experiments representative of current observational capabilities. For standard candle bursts, f_d represents the fraction of bursts (characterized by the BATSE sample) that can be detected at a flux level $(z/R_{\rm samp})^2$ relative to the BATSE threshold and thus represents the sensitivity of the given instrument relative to BATSE for the BATSE burst population. f_d is calculated by folding a sample of BATSE bursts with time profiles drawn from the first 420 BATSE detections, and spectra drawn from a sample of 54 bright bursts measured by the spectroscopy detectors (Band et al. 1993) through the instrument response. The same bursts are folded through the BATSE instrument using the three BATSE trigger timescales, response matrices provided by the BATSE team, and average measured LAD background spectra, yielding for each burst a sensitivity relative to BATSE. For a given $R_{\rm samp}$ and z, this determines the fraction of the sample falling above the detection threshold. The most favorable detection case is assumed for BATSE, corresponding to a burst located at an off-axis position equidistant between two detectors. (BATSE requires detection above threshold in more than one detector to trigger on a burst.) For instruments other than BATSE, integration times of 2, 10, and 50 s were used, as this optimizes sensitivity for the largest fraction of bursts.

4.1.1. *Focusing Telescopes: ROSAT and ASCA*

Current generation focusing telescopes are limited to energies $\lesssim$10 keV. The principal difficulty in estimating their sensitivity to GRBs is the unknown burst X-ray spectrum. The largest sample of low-energy measurements is from *Ginga* (Yoshida et al. 1989), which detected 24 GRBs in the 1.5–10 keV band. Due to uncertainty in the incidence angle (the detector had no localization capability) and limited statistics, spectra could be obtained for only a few of these bursts. The ratio of the energy flux in the 1.5–10 keV band to that in the 1.5–375 keV band varied between 3% and 9% (with the exception of one anomalously soft burst), with an average of 5%. For the sample of bursts used here, extrapolating to 1.5 keV yields a corresponding energy flux ratio of 3.5%, consistent with the *Ginga* measurements given the limited burst sample. Thus the best assumption which can be made is smooth extrapolation of the BATSE spectra to ~1 keV. Two of the *Ginga* bursts showed X-ray emission of longer duration than the harder part of the burst. Since the ubiquity of this extended emission is not established, we take the X-ray duration to be equal to that measured in gamma rays.

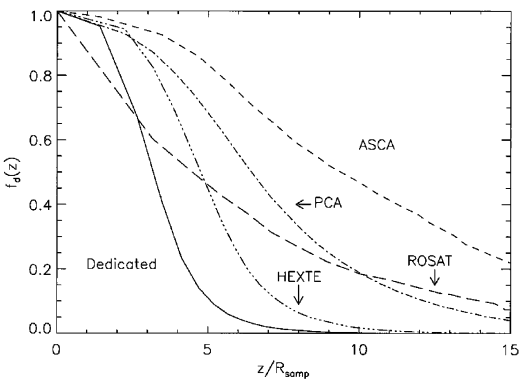

FIG. 1.—Fraction of bursts falling above the on-axis instrument detection threshold, f_d, as a function of line-of-sight distance divided by the BATSE sampling distance, $z/R_{\rm samp}$ for various instruments.

Assuming a lower energy cutoff of 1 keV, f_d as a function of $z/R_{\rm samp}$ for *ROSAT* and the combined *ASCA* gas imaging spectrometers (GIS) is shown in Figure 1. For these instruments the detection threshold is flux limited, and we have set a requirement of five photons in a detection cell. The background per detection cell is negligible (0.02 counts s^{-1} for the combined GIS), and this is adequate to avoid statistical fluctuations. However, artifacts in the *Einstein* IPC mimicking bursts have been reported (Hamilton, Gotthelf, & Helfand 1995), and more photons may be required to reject these spurious events. The higher sensitivity of *ASCA* is due to the larger energy band (1–12 keV), as compared to *ROSAT*, which has response only up to 2.4 keV.

4.1.2. *Collimated, Shielded Instruments: X-Ray Timing Explorer (XTE)*

The PCA experiment on *XTE* is a large area (~5000 cm^2 at 10 keV) instrument with low internal background, which is collimated to a 1° FOV, and operates in the 2–60 keV band (Glasser, Odell, & Seufert 1994). At the peak of the instrumental efficiency curve at 10 keV, the total background flux is a factor ~20 lower than the BATSE background at 100 keV (near the peak of the BATSE efficiency). Burst fluxes at 10 keV are typically a factor of 10 larger than at 100 keV (with ratios for our sample of bursts ranging from 0.1 to 50), leading to higher detection sensitivity. As the photons can be individually time tagged, and temporal variations in the background count rate on timescales of 1 minute are small, the longer integration intervals described in § 4 can be used. Figure 1 shows f_d for the PCA. The burst spectra are extrapolated to 2 keV, and a trigger threshold of 5.5 σ has been adopted (giving fewer than one false detection due to statistical fluctuations in a search interval of 1 yr).

TABLE 1

EXPECTED DETECTION RATES PER YEAR AS A FUNCTION OF R_{samp}

	ASCA (FOV 0.°4)		*ROSAT* (FOV 2.°0)		PCA (FOV 1°)		HEXTE (FOV 1°)		DEDICATED (FOV 18°)	
R_{samp}	High	Low	High	Low	High	Low	High	Low	High	Low
150	5	2.6	20	10	7.6	3.9	3.5	1.8	73	72
250	6	2.9	30	14.5	11	5.4	10	4.7	268	215
350	2.4	0.75	15	4.7	5.0	1.6	4.9	1.5	504	343
Control	0.18		0.75		0.25		0.14		24	

The HEXTE experiment on *XTE* consists of eight collimated (1° FOV), actively shielded NaI detectors each with 200 cm^2 geometric area operating in the 15–200 keV band. These detectors have a total background a factor $\gtrsim$40 lower than BATSE in the 50–100 keV band. The energy range of these detectors extends to 15 keV. The calculated sensitivity distribution for HEXTE is shown in Figure 1, showing that HEXTE detects more than 50% of bursts a factor of 20 fainter than BATSE. The search threshold for HEXTE is set to 5.5 σ.

4.1.3. *Dedicated Instrument*

As demonstrated by consideration of *XTE* instrument sensitivities, a collimated, shielded experiment with moderate collecting area, covering an energy range in which burst spectra are well known (10–200 keV) can detect a significant fraction of the BATSE burst sample a factor $\gtrsim$30 fainter than BATSE. Since the burst density enhancements for nearby galaxies subtend large regions on the sky (a 200 kpc burst corona around a galaxy at 1 Mpc extends over 400 deg^2) optimizing detection rates for nearby galaxies suggests, for similar configurations to HEXTE, sacrificing some sensitivity for a wider FOV. For a fiducial experiment with 2500 cm^2 collecting area, internal background of 2×10^{-4} counts cm^{-2} s^{-1} keV^{-1} (similar to HEXTE), diffuse background contribution scaled to 225 deg^2 FWHM FOV and spectral coverage in the 10–150 keV band (with detector quantum efficiency consistent with HEXTE) the expected sensitivity distribution is plotted in Figure 1. Although f_d is smaller than for the other instruments represented, the burst detection rate is higher due to the larger FOV.

4.2. *Expected Detection Rates*

We have calculated the burst detection rate from M31 for the instruments considered above. In equation (4) we use $\epsilon_{obs} = 0.7$, $M = 2$, and $N_G = 1200$ (the number of bursts above the BATSE threshold when detector efficiencies are factored in) and numerically integrate over the model halo to find F_D. Table 1 summarizes the expected detection rates per year as a function of R_{samp}. The minimum and maximum values indicate, for a given R_{samp} the minimum and maximum rates for the range of model parameters (varying r_c and α) consistent with the BATSE data. Also indicated in the table is the number of bursts expected in a control field, calculated by extrapolating the BATSE number–flux relationship to the instrument threshold. This should yield an upper limit to the background burst rate. For all instruments considered, a significant fraction of M31 bursts fall above the sensitivity threshold for values of R_{samp} in the range 150–400 kpc; however, with the exception of the dedicated experiment, the limited instrument fields of view lead to prohibitively long observation times. In most cases, even a year is not sufficient to detect excess bursts from M31 above the background. For the dedicated instrument, the required observation time is on the order of 8 months (four on-source + four control field) for a 5 σ (worst case) detection.

For the focusing telescopes and the PCA, observations of galaxies out to several megaparsecs are possible. The projected burst halos of more distant galaxies will be smaller and hence the burst contrast higher. For example, a 250 kpc burst halo surrounding M81, a massive spiral at a 3.6 Mpc would subtend 50 deg^2 on the sky. However, the burst detection efficiency at this distance is smaller and the total detection rate for *ASCA* or *ROSAT* comparable to the rates for M31. Galaxies more distant than this rapidly become undetectable.

5. CONCLUSION

Until the order of magnitude of the GRB distance scale is known, detailed theoretical burst models can be only speculative at best. The clearest distinction between galactic and extragalactic source models is the prediction of galactic models that burst halos should exist around neighbors of the Milky Way. As BATSE has failed to detect an excess of bursts toward M31, it is clear that a more sensitive instrument is required. Unfortunately, the small fields of view of existing satellites make them unsuitable for detection of the low surface-brightness features in the burst distribution in reasonable observation times. However, a small satellite optimized for burst measurements could detect the halo of M31 for any values of the parameters of such a halo that are allowed by the isotropy measurements of BATSE.

We thank the members of the Andromeda Science Working Group (B. Paczyński, D. Chakrabarty, W. R. Cook, C. Hailey, T. T. Hamilton, D. W. Hogg, S. R. Kulkarni, W. H. G. Lewin, P. Podsiadlowski, T. A. Prince, P. S. Ray, S. M. Schindler, and H. Tannenbaum) for their contributions to this work. F. A. H. acknowledges support from a Robert A. Millikan Fellowship.

REFERENCES

Band, D. L., et al. 1993, ApJ, 413, 281
Chuang, K. W., White, R. S., Klebesadel, R. W., & Laros, J. G. 1992, ApJ, 391, 242
Cohen, J. 1985, ApJ, 292, 90
Fenimore, E. E., & Bloom, J. S. 1995, ApJ, 453, 25
Fishman, G. J., et al. 1994, ApJS, 92, 229
Glasser, C. A., Odell, C. E., & Seufert, S. E. 1994, IEEE Trans. Nucl. Sci., 41, 1343
Hakkila, J., Meegan, C. A., Pendleton, G. N., Fishman, G. J., Wilson, R. B., Paciesas, W. S., Brock, M. N., & Horack, J. M. 1994, ApJ, 422, 659
Hamilton, T. T., Gotthelf, E., & Helfand, D. J. 1995, preprint
Klebesadel, R. W., Strong, I. B., & Olson, R. A. 1973, ApJ, 182, L85
Lamb, D. Q. 1995, PASP, in press
Liang, E. P. 1991, ApJ, 380, L55
Paczyński, B. 1995, PASP, in press
Podsiadlowski, P., Rees, M. J., & Ruderman, M. 1995, MNRAS, 273, 755
Yoshida, A., et al. 1989, PASJ, 41, 509